

# Airborne Radar Observations of Eye Configuration Changes, Bright Band Distribution, and Precipitation Tilt During the 1969 Multiple Seeding Experiments in Hurricane Debbie<sup>1</sup>

**PETER G. BLACK**—National Hurricane Research Laboratory, Environmental Research Laboratories, NOAA, Miami, Fla.

**HARRY V. SENN and CHARLES L. COURTRIGHT**—Radar Meteorology Laboratory, Rosenstiel School of Marine and Atmospheric Sciences, University of Miami, Coral Gables, Fla.

**ABSTRACT**—Project Stormfury radar precipitation data gathered before, during, and after the multiple seedings of the eyewall region of hurricane Debbie on Aug. 18 and 20, 1969, are used to study changes in the eye configuration, the characteristics of the radar bright band, and the precipitation tilt. Increases in the echo-free area within the eye followed each of the five seedings on the 18th, but followed only one seeding on the 20th. Changes in major axis orientation followed only one seeding on the 18th, but followed each seeding on the 20th. Similar studies conducted recently on unmodified storms suggest that such changes do not occur naturally. However, the studies do not exclude this possibility. Changes in the

radius of maximum winds follow closely the changes in eyewall radius. It is suggested that the different results on the 2 days might be attributable to seeding beyond the radius of maximum winds on the 18th and inside the outer radius of maximum winds on the 20th.

The bright band is found in all quadrants of the storm within 100 n.mi. of the eye, sloping slightly upward near the eyewall. The inferred shears are directed outward and slightly down band with height in both layers studied. The hurricane Debbie bright band and precipitation tilt data compared favorably with those gathered in Betsy of 1965 and Beulah and Heidi of 1967.

## 1. INTRODUCTION

On Aug. 18 and 20, 1969, the first multiple seeding of a hurricane was carried out in hurricane Debbie. Freezing nuclei (silver iodide) were injected into the hurricane along a 15- to 25-n.mi. swath beginning at the inner edge of the northeast sector of the eyewall and extending outward at an altitude of 35,000 ft ( $-25^{\circ}$  C). Seeding was repeated five times at intervals of 2 hr.

The Stormfury experiment was designed to test the hypothesis that seeding the clouds radially outward from the inner edge of the eyewall (near the radius of maximum winds) would cause a reduction and outward displacement of the maximum winds by releasing large amounts of latent heat, causing a pressure fall beneath the seeded region, and lessening the pressure gradient. An earlier and similar hypothesis was outlined by Simpson et al. (1963) but was subsequently modified by Gentry (1969).

Examination of recent numerical modification experiments by Rosenthal (1971) has led to a different hypothesis. The new hypothesis has resulted from the exchange of ideas by several people and is still being checked and improved. As summarized by Gentry (1971), it suggests that seeding the hurricane beyond the radius

of maximum winds will cause the cumulus towers at radii from about 5 to 30 n.mi. from the inner edge of the eyewall to grow, thus building a new eyewall at a larger radius.

The Stormfury Operations Plan (U.S. Navy Fleet Weather Facility 1969) has described in detail the flight patterns that were carried out by the NOAA-Research Flight Facility (RFF), Navy, and Air Force aircraft involved in the monitoring of the storm before, during, and after the seeding operation. Gentry (1970) and Hawkins (1971) have described the results from the wind, temperature, etc., data collected by some of these aircraft. Their results were generally in the sense predicted by the new hypothesis.

Another approach to the problem of proving or disproving this hypothesis is taken in this paper. Sheets (1970) has examined flight data collected in hurricanes by RFF aircraft during the past 10 yr. He has concluded that, for mature hurricanes, the radius of maximum winds was most likely to be located about 3 n.mi. radially outward from the inner edge of the eyewall. In addition, Rosenthal (1971) has suggested that, in a steady-state mature storm, the position of the eyewall should be well correlated with the radius of maximum winds. Therefore, the radar data collected during the experiment were examined in an effort to detect changes in the eyewall region that could be related to the seeding. Unfortunately, because of a lack of high quality data, de-

<sup>1</sup> Contribution No. 1402 from the University of Miami, Rosenstiel School of Marine and Atmospheric Sciences

finite results were not entirely possible. Nevertheless, two studies were decided upon. One was to document the time variation of the eye configuration during the seeding operations on August 18 and 20 (data were available for only 1 hr before until 1 hr after the seeding period on each day). The other was to document the bright band height and thickness as well as the precipitation tilt on August 20.

The objective of the eye size study was to look for evidence to suggest an outward displacement and, hence, weakening of the maximum wind region, as predicted by the Stormfury hypothesis. Such an outward displacement was reported by Simpson and Malkus (1964), who stated that at some time after the single seeding attempt on hurricane Beulah on Aug. 24, 1963, the eye increased in radius from about 10 n.mi. to about 20 n.mi. However, at that time, they were not certain whether or not the fluctuations were natural or were changes caused by seeding.

Although occasional observations of bright bands in small segments of hurricanes date back to 1945 (Atlas et al. 1963), Senn (1966b) showed that this phenomenon was observed in almost all regions of hurricane Betsy of 1965. Unfortunately, it is not generally possible to make widespread observations of the bright band in most hurricanes because of the path of the storm, the lack of high quality, narrow beamwidth range-height indicator (RHI) radars, and/or the lack of qualified observers to man the airborne RHI radars in non-Stormfury reconnaissance missions. The present data on Debbie, therefore, constitute another attempt to study such conditions simultaneously throughout a hurricane.

For the same reasons, precipitation tilt data from RHI radars throughout hurricanes are rare. In a previous paper, Senn (1966b) showed that tilt observations were often dismissed as erroneous or due to equipment problems when, in fact, they were probably real. A careful check of the equipment and analysis of the data from hurricane Betsy confirmed the validity of the observations of appreciable tilt at most levels and azimuths in that storm. The same equipment and basic methods were used to obtain the Debbie data during the Project Stormfury experiments.

## 2. RADAR DATA INTERPRETATION PROBLEMS

The Operations Plan (U.S. Navy Fleet Weather Facility 1969) called for over 20 plan-position indicator (PPI) radarscopes to be photographed once every 10 s, and the four prime RHI radarscopes to be photographed once every 3–5 s. The characteristics of the radars used in this study are given in table 1. Less than 20 percent of the anticipated PPI data and less than 10 percent of the anticipated RHI data were considered usable for this research due mainly to below-normal performance of the radars, lack of antenna stabilization, range attenuation effects in the shorter wavelength radars, and poor azimuth documentation. These effects made it difficult to establish continuity on the various eyewall features, a process that

TABLE 1.—*Characteristics of radars used for eye configuration study*

	APS-20*	APS-45*	APS-64†	WP-101‡
Wavelength	10 cm	3.2 cm	3.2 cm	5.5 cm
Peak power	2 Mw	450 Kw	40 Kw	75 Kw
Beamwidth (horizontal/vertical)	1.5°/5.5°	3.1°/1.0°	1.5°/csc <sup>2</sup>	7.5°/7.5°
Pulse length	2 $\mu$ s	1.8 $\mu$ s	2.5 $\mu$ s	2.1 $\mu$ s
Pulse repetition frequency	270 s <sup>-1</sup>	450 s <sup>-1</sup>	200 s <sup>-1</sup>	400 s <sup>-1</sup>

\* WC-121N, Weather Reconnaissance Squadron Four, U.S. Navy

† WB-47, 53d Weather Reconnaissance Squadron, U.S. Air Force

‡ DC-6, Research Flight Facility, NOAA

was made more difficult by the rapidly changing nature of the eyewall itself.

A comparison of the eyewall region in figure 1B with the eyewall region in the radar composite constructed by Fujita and Black (1970) using the 3-cm APS-64 radar will demonstrate some of the problems encountered due to range attenuation when using short wavelength radars.

In an attempt to minimize these problems, two methods of measuring the echo-free eye area were used. One method consisted of planimetering the echo-free eye region. The other method consisted of measuring the major and minor axes of the eye and computing its area from the ellipse formula. The two measurements were made independently by different people. There were periods when the echo-free eye was especially difficult to define and at these times there were disagreements between the two methods. In these data-poor regions, it is thought that measuring major and minor axes provided a more reliable measure of the eye size than did the planimetered area.

A considerable number of calibration problems were also encountered. By analyzing ground targets after take-off and before landing, researchers found that many of the radars have range mark errors up to 10 percent and north-line errors of up to 25°. This complicated the eye size analysis. However, during most of the period of study, there were simultaneous data available from two radars and, for short periods of time, from up to four radars. After the calibrations were made, the data taken from different radars at the same time produced consistent results.

## 3. QUALITATIVE RADAR FEATURES OF HURRICANE DEBBIE

Figure 1 shows a representative PPI display of hurricane Debbie on each of the two operational days. Since there was no single high-quality photograph of the storm, figure 1 is a composite constructed from photographs taken over a period of several minutes centered on the indicated time. Only the 10-cm APS-20 radar photographs were used. Figure 1 illustrates the basic difference in the storm on the 2 days. On the 18th, only a single wall cloud was evident, except for occasional periods when a second, concentric wall cloud was attempting to

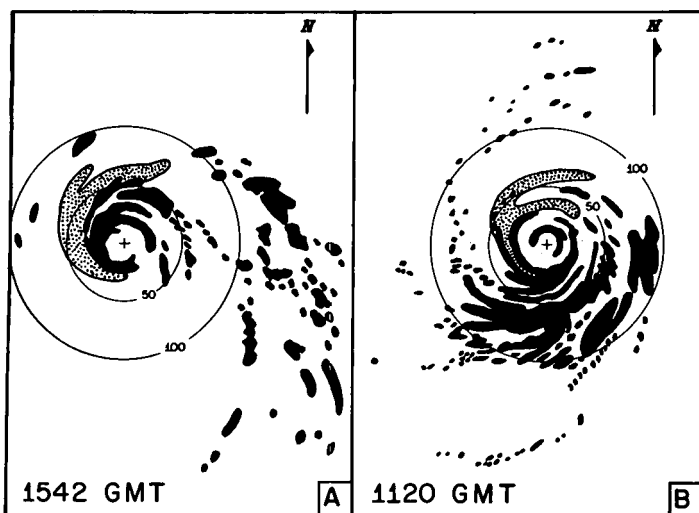


FIGURE 1.—Typical APS-20, 10-cm radar composites of hurricane Debbie on (A) Aug. 18 and (B) Aug. 20, 1969. The dotted areas indicate regions of faint echoes.

form. However, on the 20th, concentric wall clouds were evident for the entire day. On the 18th, the storm was more asymmetric than on the 20th with numerous precipitation echoes in a large band extending to the east and southeast of the center. The most intense precipitation echoes were located in the north and northeast quadrant while there was none outside the eyewall to the southwest and south. The southeast quadrant of the eyewall was open most of the day.

On the 20th, Debbie appeared to have a more uniform distribution of echoes around the storm. Figure 1B does not show all the echoes to the north of the storm that were observed later in the day, for reasons stated in the previous section. Nevertheless, a fair idea of the echo distribution can be shown. The outer eyewall was closed during the entire day and was generally more solid than the inner eye, which was often broken in appearance especially in the south quadrant. Again, the most intense precipitation was located in the northeast quadrant.

The concentric wall cloud structure, or “double eye” as it is sometimes called, is apparently not an uncommon feature of hurricanes or typhoons. Fortner (1958) first described this feature in typhoon Sarah of 1956, and later Jordan and Schatzle (1961) reported a double eye in Hurricane Donna of 1960. Many other cases are described in the Annual Typhoon Reports prepared by the Joint Typhoon Warning Center on Guam. However, the double eye is usually associated with more intense storms than Debbie.

Figure 2 shows the distribution of the maximum echo heights in each quadrant of the eyewall on both days as estimated from the available APS-45, RHI data. One can see that on the 18th the maximum echo heights were lowest in the southwest quadrant (averaging 25,000–30,000 ft) and highest (averaging 45,000 ft) in the northeast quadrant. A similar picture is evident from the data on the 20th with the lowest maximum echo heights (averaging 30,000 ft) being located in the southwest quadrant

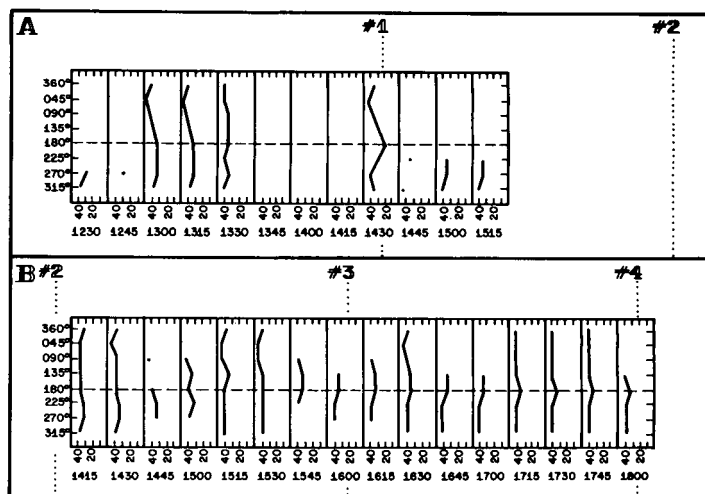


FIGURE 2.—Maximum height ( $10^3$  ft) of radar echoes in each quadrant of the hurricane Debbie eyewall on (A) August 18 and (B) August 20, obtained from the 3-cm APS-45 radar. The vertical dotted lines indicate the seeding times and are numbered relative to the first seeding. All times are GMT.

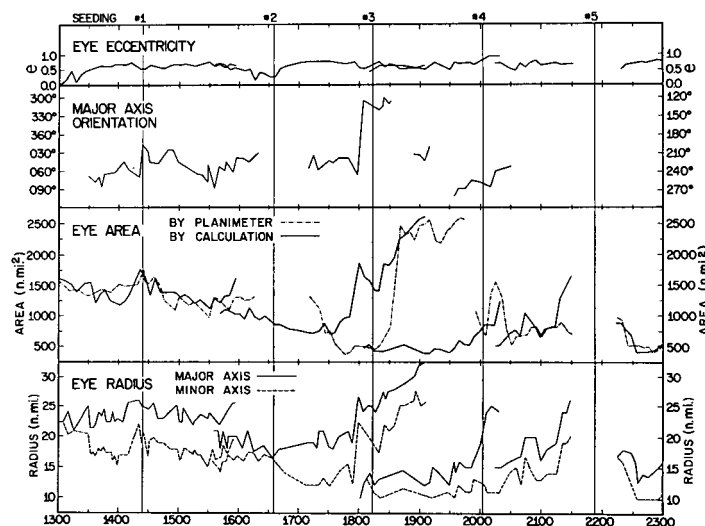


FIGURE 3.—Eye configuration changes in hurricane Debbie from 1300 to 2300 GMT on August 18. Vertical lines indicate the seeding times.

early in the day, shifting to the southeast later in the day. The highest echoes (averaging 45,000 ft) were again located in the northeast quadrant. Echo tops in hurricane Donna, although at greater ranges, were also higher to the right of the storm center (Senn and Hiser 1962).

It is interesting to note that, despite the different radar configuration of Debbie on the 2 days, the maximum wind at 12,000 ft on both days before seeding was nearly the same, approximately 100 kt (Gentry 1970).

#### 4. EYE STRUCTURE CHANGES ON AUG. 18, 1969

Figure 3 shows the changes in eye radius, echo-free area, major axis orientation, and eccentricity that occurred just prior to, during, and immediately following the multiple seedings, which are shown by vertical lines at

seeding times. The planimetered area is indicated by the dot-dashed line and the area computed from the measured radii is given by the solid line.

Eye size changes on the 18th were much more pronounced than on the 20th. Unfortunately, radar data quality was poorer on the 18th. The data from 1500 GMT to 2000 GMT are considered most reliable because they consist of an average of measurements from two and sometimes three radars.

Careful study of figure 3 leads to the following observations. Approximately 1 hr and 15 min after the first seeding, the eye area began to increase rapidly. During a period of 30 min, the eye increased in area by 50 percent until it disappeared, and a new eye formed. Again, approximately 1 hr after the second seeding, a rapid increase in the area occurred. This time, the area nearly tripled in a period of 15 min. The increase does not appear in the planimetered area due to a difference in interpretation of the echoes which made up the eyewall while it was in the process of re-forming. Just prior to the third seeding, a double eye structure clearly appeared. The larger eye continued to increase in area following the third seeding until it disappeared approximately 1 hr after the seeding. Meanwhile, the smaller eye slowly increased in area. Shortly after the fourth seeding the eye area again increased suddenly and disappeared. A smaller eye quickly re-formed and slowly began to increase in area until about 1 hr and 15 min after the fourth seeding when another sudden increase in area occurred. In that case, the area doubled in size in about 10 min. A larger increase may have occurred, but lack of data prevented further measurements until shortly after the fifth seeding. At that time, the data showed that a smaller eye had formed. No further data were available after 2300 GMT.

The manner in which the sequence described above occurred is difficult to ascertain exactly because of poor definition in the radar photographs of the wall clouds. However, a schematic illustration of the process as it occurred following the third seeding is shown in figure 4. Each of the six views represents a composite of several radar film frames centered on the indicated time. Apparently the echoes in the northern and southern segments of the eyewall began moving outward, as shown in the sequence of sketches from 1730 to 1753 GMT. At about 1753, a protrusion in the western segment of the eyewall began moving inward rather quickly. As this movement continued and the echoes spiraled inward, a new and smaller wall cloud was formed as can be seen in the sequence of sketches from 1753 to 1820 GMT. Meanwhile, the northern segment of the original eyewall appeared to break up into smaller echoes as it moved outward and lost its identity while the southern segment moved outward and merged with a feeder band. This process is believed to be representative of what happened following the other seedings. However, this cannot be proven conclusively due to the poor quality of the data.

The eye retained its elliptical shape during the day with an average eccentricity of about 0.7. The northeast to southwest orientation of the major axis remained nearly

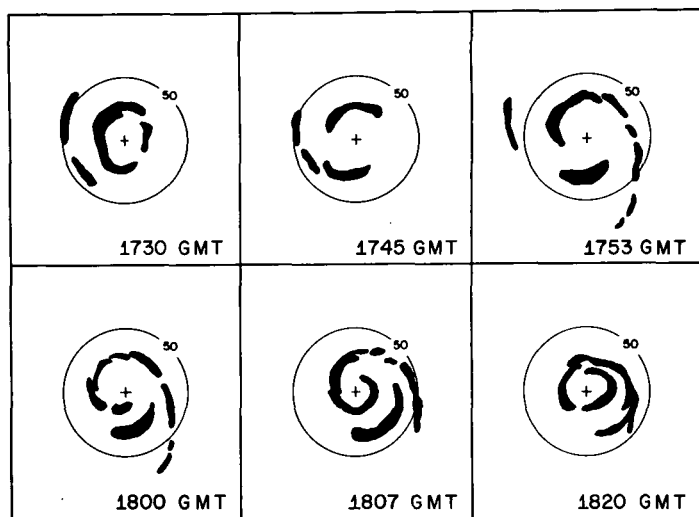


FIGURE 4.—Process of eyewall expansion as it occurred after the third seeding of hurricane Debbie on August 18. North is toward the top of each panel.

constant for most of the day with the exception of a sudden change between 1800 and 1900 GMT, the time during which the largest expansion of the eyewall occurred.

## 5. EYE STRUCTURE CHANGES ON AUG. 20, 1969

The changes in eye radius, echo-free area, major axis orientation, and eccentricity on Aug. 20, 1969, shown in figure 5, are more subtle than on the 18th. As was noted earlier, two concentric wall clouds existed on this day as opposed to a single wall cloud on the 18th. The larger eye had a mean radius of 22 n. mi. while the smaller, inner eye had a mean radius of 12 n. mi.

The radar data quality was much better on the 20th than on the 18th, although far from optimum. As on the 18th, data exist only from 1 hr before the first seeding until 1 hr after the last seeding. From the second through the fourth seeding, two, three, and sometimes four radars were used to obtain measurements. All agreed rather well; this heightened confidence in the measurements.

The first four seedings were conducted on the inner eyewall, but the last seeding was conducted on the outer eyewall. The areas and radii of the large and small eyes showed only minor changes after each seeding. The following features are noteworthy. The area of the large eye showed a general trend to decrease in size during the day. The area of the small eye remained nearly constant until 1900 GMT when it began a slight increase, resulting in a much reduced separation between the two wall clouds by the end of the seeding operation. The eccentricity of the two eyes did not change markedly during the day, the outer eye having a mean value of about 0.4 and the inner eye, being more elliptical, having a mean value of about 0.6.

The behavior of the major axis orientation was also different on the 20th than on the 18th. On the 20th, the axis did not remain fixed as it did on the 18th, but rotated.

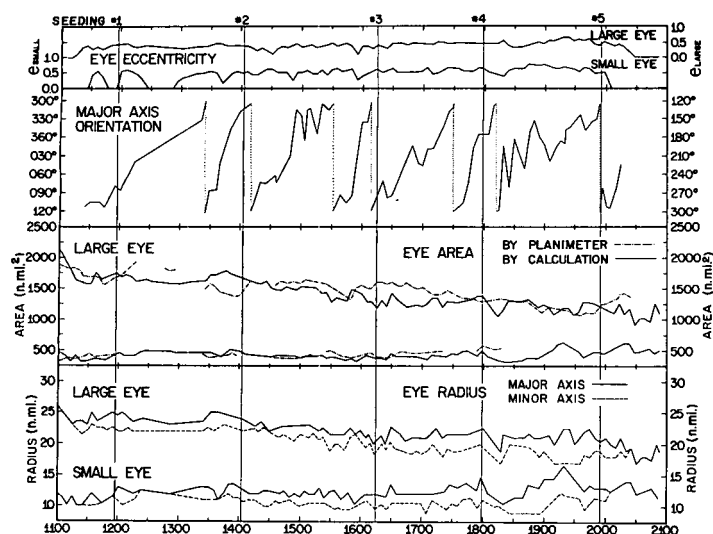


FIGURE 5.—Eye configuration changes in hurricane Debbie from 1100 to 2100 GMT on August 20. Vertical lines indicate the seeding times.

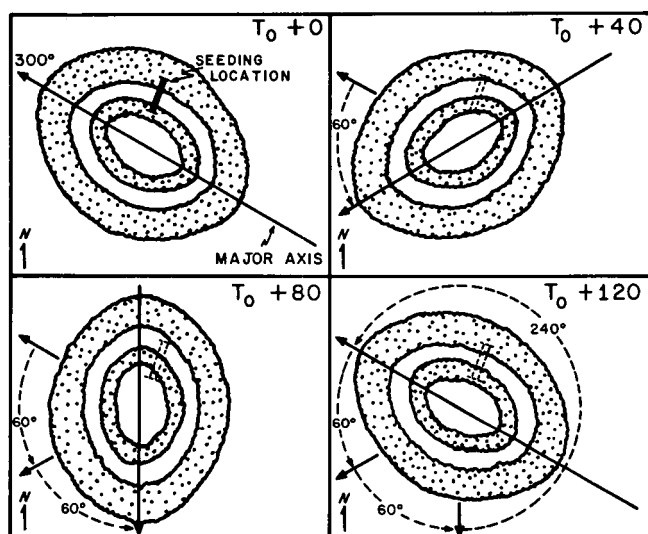


FIGURE 6.—Schematic illustration of the rotational acceleration and deceleration of the eyewall major axis following each seeding of hurricane Debbie on August 20.

The interesting feature about the major axis orientation is that as it rotated it went through a definite cycle that had a period of about 2 hr. As can be seen from figure 5, four of these cycles were observed, one following each seeding. The orientation of the major axis was northwest to southeast at each seeding time, the seedings taking place in the direction of the minor axis.

Figure 6 illustrates schematically the rotation cycle of the eyewall. Beginning shortly after each seeding, the rotation rate of the major axis decelerated so that during the first 40 min after seeding it had rotated through only 60°, a rate which continued for the next 40 min. Then rapid acceleration took place so that within the next 40 min the major axis rotated through nearly 240° before decelerating again. Thus, it appears that one effect of seeding was to slow the rotation rate of the major axis of

TABLE 2.—Comparison of changes in radar eye radius with changes in the radius of maximum wind on Aug. 18, 1969

Time (GMT)	Wind profile orientation	Major axis orientation	Wind max. radius (n.mi.)	Radar eye radius (n.mi.)
1300–1600 (along major axis)	040°–220°	050°–230°	22	23
1600–1700 (along minor axis)	120°–300°	050°–230°	20	17
1800–1830 (along minor axis)	040°–220°	120°–310°	25	11, 21
1830–1900 (along major axis)	040°–220°	040°–220°	30	14, 30
1900–2000	040°–220°	070°–250°	20	15

TABLE 3.—Comparison of changes in radar eye radius with changes in the radius of maximum wind on Aug. 20, 1969

Time (GMT)	Wind profile orientation	Major axis orientation	Wind max. radius (n.mi.)	Radar eye radius (n.mi.)
1130–1230 (in between axes)	020°–200°	070°–250°	11, 24	12, 24
1450–1500 (along minor axis)	120°–300°	050°–230°	11, 22	11, 22
1830–1930 (along major axis)	020°–200°	030°–210°	14, 21	14, 21

the elliptical eyewall. Although the rotation of the major axis of an elliptical eye was thought to be indicative of changes in the storm track in hurricane Donna (Sadowski 1961), Senn (1966a) found such rotation occurring in other storms without track changes.

## 6. COMPARISON OF EYEWALL RADIUS CHANGES WITH CHANGES IN THE MAXIMUM WIND RADIUS OBSERVED IN HURRICANE DEBBIE

The process of eye expansion and re-formation is supported to some extent by the behavior of the winds at 12,000 ft on the two seeding days that were monitored by the RFF, DC-6 aircraft and reported by Gentry (1970) and Hawkins (1971). Tables 2 and 3 summarize the comparisons between the orientation of the aircraft passes, the orientation of the major axis of the eye, the radius of maximum wind, and the radar eye radius on the 18th and 20th, respectively.

Tables 2 and 3 show a high degree of correlation between the fluctuations in the radius of maximum winds and the eyewall radius along the aircraft track, certainly within the limits of aircraft navigation errors. In general, the eyewall radius is equal to or slightly less than the radius of maximum winds, indicating that the centers of the eyewall and maximum wind region are nearly coincident. The data in table 2 indicate that as the eyewall expands and contracts on the 18th, so does the radius of maximum winds. The data in table 3 show that both the larger

eyewall radius and the larger maximum wind radius are decreasing with time on the 20th. As noted earlier, the data in Figure 5 show the inner and outer eyewalls coming closer together with time. Not shown in table 3 is that at a later time, about 5 hr after the seedings had ended, the inner wind maximum had been eroded away and only a single maximum existed at a radius of about 20 n.mi. Therefore, the fluctuations in the radius of maximum wind on both days tend to support the fluctuations in the radar eyewall radius.

It is interesting also to compare the changes in eyewall radius with recent numerical modification experiments carried out by Rosenthal (1971). In his experiments, he used a circularly symmetric model (Rosenthal 1970) with continuous enhanced heating (to simulate the effect of seeding) beyond the radius of maximum winds for a period of 10 hr. Comparisons with intermittent seeding in a real asymmetric storm are, therefore, difficult. Nevertheless, it is significant that the maximum wind region in the modified model storm began shifting outward shortly after the enhanced heating had commenced. By 2 hr after the enhanced heating had ceased, the maximum wind region had shifted from a 10- to a 20-n.mi. radius. It would appear, therefore, that the timing of the outward shifting of the radar eyewall, beginning 80 min after each seeding, is not an unreasonable response time for the storm to react to the seeding. The fact that the eyewall expansion did not continue is significant.

Perhaps in future seeding experiments the seedings should be repeated more frequently and at successively larger radii as the eyewall expands. In this way, possibly the eyewall and the maximum wind region could be maintained at a larger than natural radius and thus prolong the reduction in wind speed.

## 7. EYE SIZE CHANGES IN UNSEEDED STORMS

The question may be asked whether or not eye size changes described previously would have occurred if the storm had not been seeded. Hoecker and Brier (1970) have conducted a study of the eye size changes in Hurricanes Carla of 1961, Betsy of 1965, and Beulah of 1967, covering a continuous time period of about 24 hr for each storm. Airborne radar was used only for the Carla study, while ground based radar was used for all three storms.

The data sample for Carla was the longest (40 hr). For this storm, the eye decreased in size from a 30 n.mi. diameter to 23 n.mi. diameter during the first 24 hr and remained relatively constant thereafter. Superimposed upon this trend were shorter period fluctuations of the order of  $\pm 4$  n.mi. in 4 hr. The Betsy and Beulah eye sizes behaved somewhat similarly. It should be mentioned that during the period of study, both Carla and Beulah had a double eye structure, while Betsy had a single eye.

In the above data sample, there was no evidence of cyclic, short period (on the order of 2 hr) changes in the eye size or shape, or even any sudden individual changes of the magnitude and time scale observed in Debbie. However, sudden significant changes in eyewall structure probably occur at some time or other in the life history of

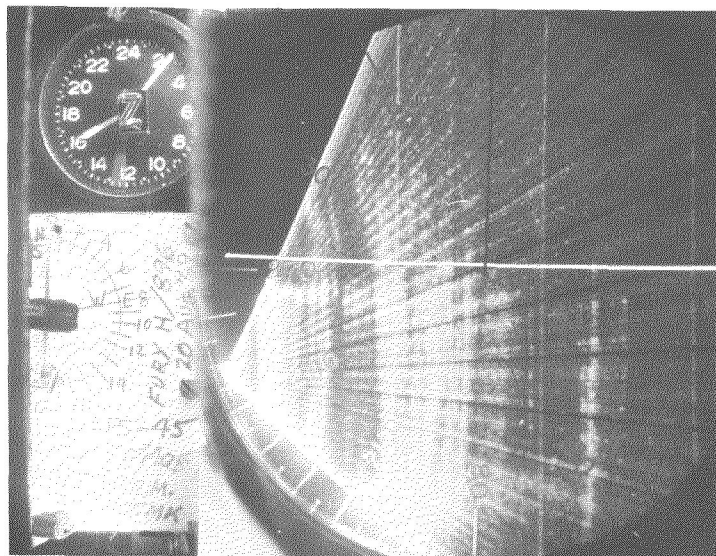


FIGURE 7.—Typical APS-45 radar photograph showing the vertical structure of radar echoes distorted 10:1 in the vertical. Vertical lines are range marks at 20-n.mi. intervals. The horizontal line is the 20,000-ft height line. The sea return can be seen as the fuzzy horizontal echo at the bottom of the photograph. The bright band is the thin band echo just below the height line. The azimuth of the photograph is indicated by the pointer beside the data card, which in this case indicates 360°.

most hurricanes. Such changes usually accompany rapid deepening or filling of the storm such as during landfall or while passing over warmer or colder than normal sea surface temperatures.

Recently, Fujita (1971) documented the eye diameter changes in hurricanes Camille of 1969 and Celia 1970 for a 7½-hr period before and just after landfall. His data showed some evidence of a cyclic change in the major and minor axis diameters beginning about 2 hr before landfall. The eye diameters were nearly constant prior to this time. Both the period and amplitude of the cycle were about one half that found in Debbie.

Therefore, the data studied by Hoecker and Brier as well as several unpublished accounts of hurricane radar observations suggest that cyclic eye size changes of the type observed in Debbie may be somewhat unique. However, further study of unseeded storms is necessary to be more certain of this.

## 8. DISTRIBUTION OF THE BRIGHT BAND IN HURRICANE DEBBIE

One of the interesting features of the APS-45 RHI photographs taken in hurricane Debbie was the frequent occurrence of the bright band. This is a region of enhanced radar reflectivity at levels just below the 0°C isotherm caused by the melting of frozen precipitation. The significance of this feature is that it can only exist in regions of weak vertical motion (less than 1 m/s). Hence, its existence in a hurricane can be used to infer regions of weak vertical motion. A typical example of the bright band is seen in figure 7. The bright band is visible at times out to a range of 30 n.mi. from the radar.



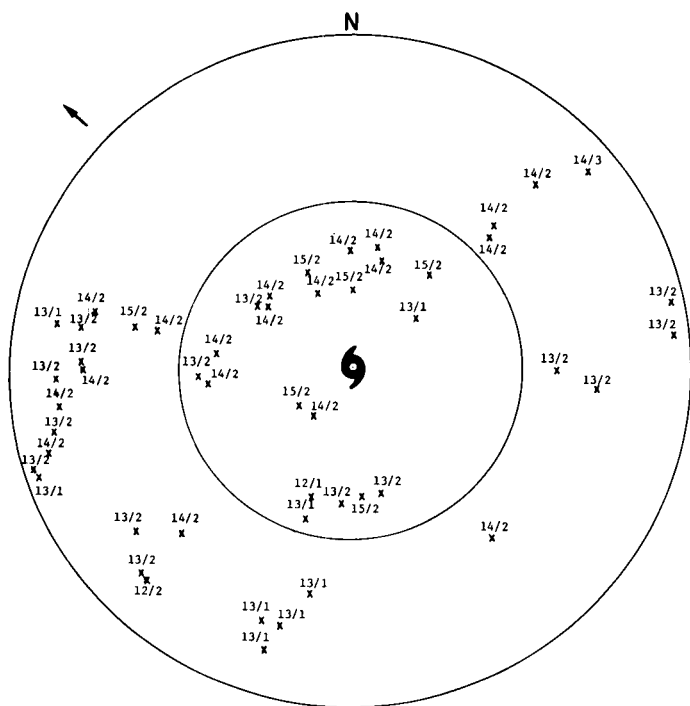


FIGURE 8.—Average bright-band heights/thicknesses ( $10^3$  ft) in hurricane Debbie from APS-45 at 1,000 ft on August 20. The arrow in the upper left in this and subsequent figures is the storm direction of motion. The range marks are at 50-n.m.i. intervals.

Figures 8 and 9 show the distribution of the bright band and its mean height and thickness as measured by APS-45 radars on two different aircraft. Lack of good stabilization of the radar antenna presented problems in analyzing the data. Although care was taken to select only those photographs where the sea return was level (indicating a properly oriented antenna platform), there was some scatter in the data.

On the early low-level flight (1,000 ft) before seeding, the RHI radar was able to detect a well-defined bright band in most quadrants of the storm (fig. 8) except for the northwest quadrant beyond about 30 n.m.i. from the storm center. Considering the number of RHI photos taken in Debbie and the concentration of the observer on specific areas of the storm for extended periods, we cannot accurately compare the areas where the bright band phenomenon is observed with those lacking this feature. However, probably 25 percent of the RHI photos indicated that a bright band was in evidence. Contrasting these values with the data obtained from the higher level flight (10,000 ft) during and after the seedings (fig. 9) in the area south of the storm center, we find that the bright bands observed from the high-level flight are higher by 3,000–4,000 ft than those from the low-level flight for unknown reasons. A small amount of overlapping data from the two flights in the southwest quadrant about 30 n.m.i. from the center at nearly the same times indicate that the height differences may be due to radar calibration. However, bright band heights and thicknesses are consistent for each radar. Due to

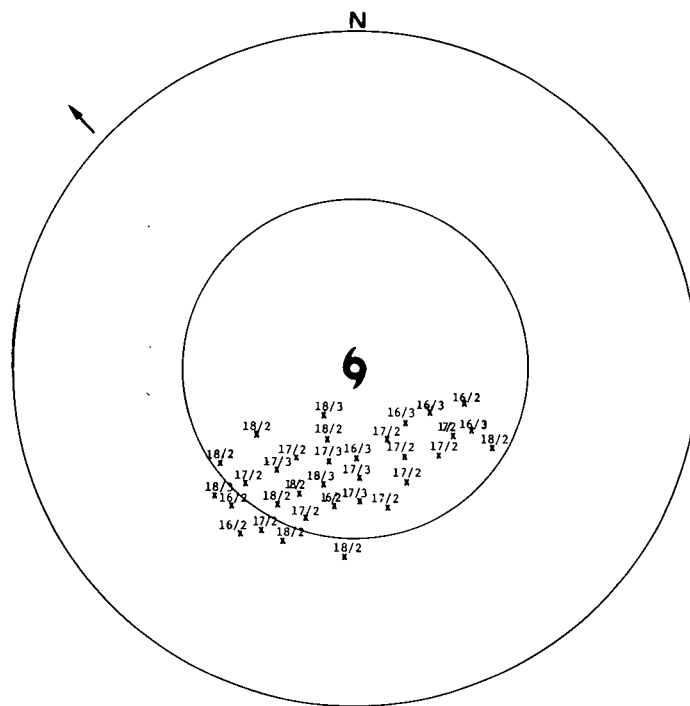


FIGURE 9.—Average bright-band heights/thicknesses ( $10^3$  ft) in hurricane Debbie from APS-45 at 10,000 ft on August 20.

radar problems on both flights, it was impossible to calibrate for height in an absolute sense; and neither operator succeeded in confirming an RHI picture of one of the Stormfury aircraft at a known altitude.

In general, the bright band appears to be 1,000–2,000 ft higher near the outer periphery of the eyewall than at the 100-n.m.i. radius. The thickness appears to be about 2,000 ft and uniform throughout the storm. The average thickness of the bright band is probably very close to the true value because it was often near the threshold of detection. It would not have suffered from even the normal beamwidth stretching of less than 1,000 ft at the short observation ranges (10–30 n.m.i.).

The  $0^{\circ}\text{C}$  isotherm was found by aircraft observations and dropsondes in various parts of Debbie to be near 15,000 ft at ranges of about 100 n.m.i. to the west, south, and southeast of the eye and was estimated to be near 17,000 ft near the eyewall. One would expect the “melting level” represented by the bright band to be topped near those levels and to extend below them. Observations from the earlier aircraft indicated the top of the bright band to be near 14,000 ft at 100 n.m.i. and about 16,000 ft near the eyewall. The later aircraft data indicated a bright band top height of 19,000 ft near the eyewall, which appears to be too high.

Comparison of the Debbie data with those obtained in Betsy of 1965 (Senn 1966b) and Beulah of 1967 shows relatively good agreement. The Beulah data were obtained at greater distances from the storm center and indicated that the average bright band height was 14,000 ft. In Betsy, the bright band also tended to be higher in and near the eyewall than at greater distances, and the phe-

nomenon was found in all azimuths and most ranges from the storm center.

The Debbie data is also in relatively good agreement with the RDR-1 RHI data of Hawkins and Rubsam (1968a, 1968b) in hurricane Hilda of 1964. The bright band was found in nearly all quadrants of the storm on three successive days. The top of the bright band was estimated to be at about 16,000 ft between radii of 50–70 n.mi. with some suggestion that the height increased near the eyewall. Hawkins noted also that convective clouds were present throughout the bright band region.

Such widespread existence of the bright band in the hurricane, which is convectively driven, raises a rather basic question. How can the bright band, which is formed by frozen precipitation falling in less than a 1 m/s updraft and melting beneath the 0°C isotherm, exist in the presence of numerous convective echoes? Atlas et al. (1963) have stated that the bright band is “characteristic of stratiform precipitation . . . and is never found in regions of strong convection.”

However, perhaps the data are not as contradictory as they may seem. The bright band observations in Debbie were frequently between the rainbands in regions of stratiform precipitation. It has been known for some time (Malkus et al. 1961) that convective bands are sometimes embedded in regions of stratiform precipitation in the hurricane. However, the bright band was also observed within convective towers in many cases. This is not too surprising, as the bright band has been observed within thunderstorms that have passed their mature stage (Battan 1959). In a hurricane, therefore, the convective towers are undoubtedly in different stages of maturity and there should be no reason why the bright band should not exist in a convective echo that is decaying, while nearby the echoes are intense and growing. In many cases, one “bubble,” or part of a convective system, is growing while another part is decaying as is clearly shown by Byers and Braham (1949). The data from both Betsy of 1965 and Debbie of 1969 show such convective echoes existing in the company of large areas of stable precipitation and bright band echo formations.

## 9. PRECIPITATION TILT IN HURRICANE DEBBIE

Another interesting measurement that can be made with the narrow beamwidth APS-45 RHI radar is the vertical tilt of the precipitation echoes. If one makes certain assumptions regarding drop sizes and fall velocities, the RHI data can be used to indicate the sense and a crude estimation of the magnitude of the wind shear in the precipitation layer observed. The echoes photographed are undoubtedly in various stages of development and hence the degree of echo tilt for a given wind shear will probably be variable, giving rise to a spectrum of inferred shears. However, the variability would be mainly in the magnitude of the shear because all the echoes should tilt to a greater or lesser degree in the direction of the shear. Even assuming a given echo is tilted significantly, only the component of tilt along the radar beam will be detected.

In fact, perhaps 75 percent of the usable RHI photographs were taken looking toward or away from the eye so that mainly the radial component of tilt was measured. Therefore, due to radar orientation as well as to meteorological reasons, only about 50 percent of the total number of echoes studied had a significant tilt (greater than 0.5 n.mi. in 15,000 ft).

It was possible to make measurements with a 0.5-n.mi. horizontal resolution and a 1,000-ft vertical resolution. Echo tilts were measured for three height intervals: surface to 16,000 ft, 16,000–30,000 ft, and above 30,000 ft. The largest data sample was in the lowest layer, where 115 tilts were measured. In the middle layer, 76 tilts were measured. Less than a dozen tilting echoes were measured in the upper layer and are not presented here. Figures 10 and 11 show the observed vector component of the precipitation tilt along the radar beam for the low and middle levels, respectively.

The average magnitude of the tilts in both layers was nearly the same, being slightly more than 1 n.mi. horizontally in 3 n.mi. vertically. This corresponds to a tilt angle of 20°. The maximum tilt measured corresponded to an angle of 45°. The direction of the tilts in the low level was generally radially outward in the front and right quadrants and generally radially inward in the left and rear quadrants. The tilt in the middle level was generally outward and slightly upband (cyclonic tangential component) in the right quadrant and outward and downband (anticyclonic tangential component) in the left, front, and rear quadrants.

The magnitude of the representative wind shear vectors in a hurricane can be roughly estimated from the precipitation tilt vectors using a procedure established by Senn (1966b). He used reflectivities obtained in hurricane Betsy from a well-calibrated radar to infer subtropical raindrop concentrations from the data of Mueller and Jones (1960). Then using the terminal fall velocity data of Gunn and Kinzer (1949) which assume the drops to be falling through stagnant air, the wind shears were computed from the APS-45 RHI tilt data. For an echo tilt of 6,000 ft in a 16,000-ft layer, the wind shear is of the order of 6 kt.

Using the precipitation tilt-wind shear relationship devised by Senn (1966b), wind shears computed from aircraft data, where available, were converted to tilts. They are plotted in figures 10 and 11 as dotted arrows. In only a few instances were aircraft at 1,000 ft coincident in space and time with aircraft at 12,000 ft and likewise, only in three cases were aircraft at 31,000 ft coincident in space and time with aircraft at 12,000 ft. Nevertheless, wind shears were computed for these few cases, but they are not considered any more reliable than the precipitation tilt-inferred shears because the low-level Navy aircraft, the middle-level RFF aircraft, and the high-level Air Force aircraft all use different navigation and wind computing schemes, none of which is calibrated with respect to either of the others.

However, fair agreement between the tilts inferred from the aircraft winds and the precipitation tilts in the lower level can be seen in figure 10. The wind shears computed from aircraft data ranged from 5 to 20 kt in the directions



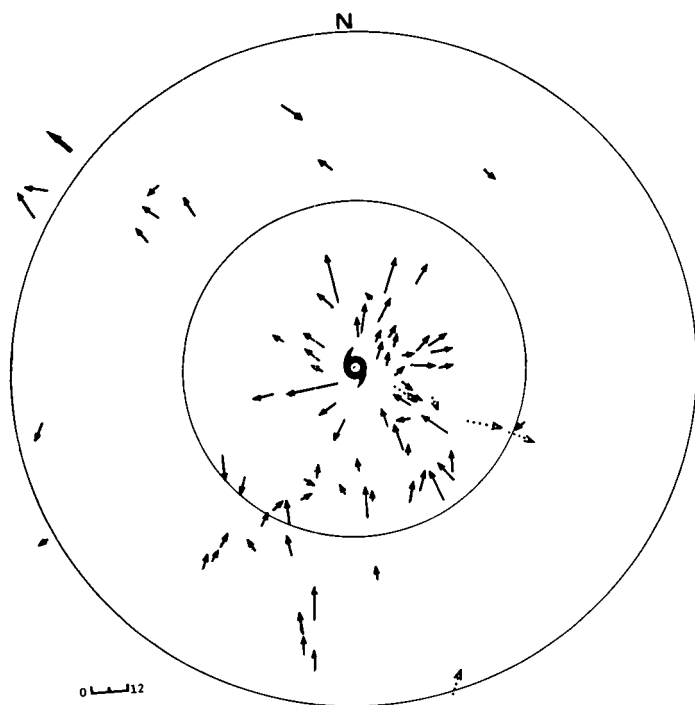


FIGURE 10.—Precipitation-tilt vector composite for the layer 0–16,000 ft in hurricane Debbie on August 20. The scale in the lower left gives the length of the echo tilt vectors in thousands of feet. The dotted arrows are tilts inferred from wind shears computed from aircraft wind measurements at 1,000 and 12,000 ft.

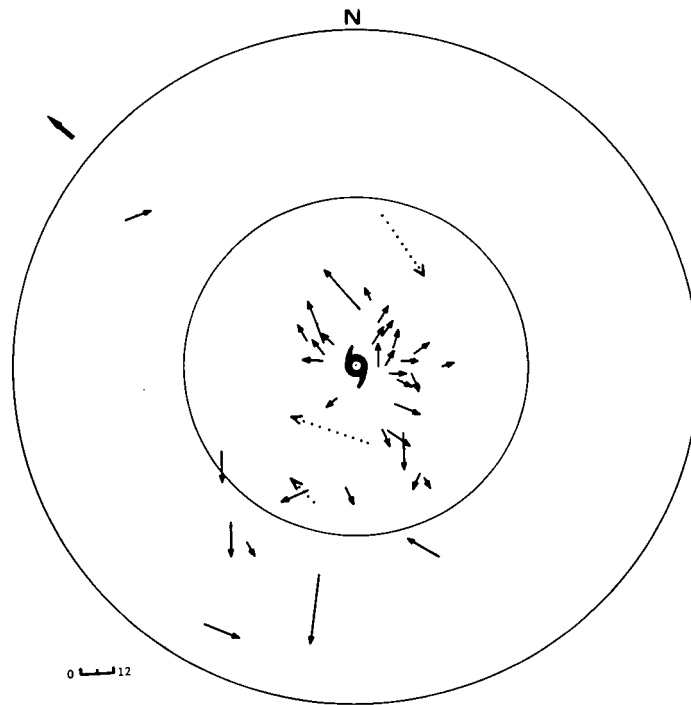


FIGURE 11.—Precipitation-tilt vector composite for the layer 16,000–30,000 ft in hurricane Debbie on August 20. The dotted arrows are tilts inferred from wind shears computed from aircraft wind measurements at 12,000 and 31,000 ft.

shown which was approximately the range in wind shear magnitude inferred from the tilt vectors in figure 10. A lesser degree of agreement is seen in the higher layer in figure 11 probably because the actual wind shears are larger in magnitude. The aircraft-derived wind shears ranged from 20 to 35 kt while the precipitation-inferred shears ranged from 5 to 20 kt.

It appears that the tilt vectors in figures 10 and 11 average about half those found by Senn (1966b) in hurricane Betsy of 1965 for an equivalent layer. The difference could be real, for Betsy was increasing from tropical storm to hurricane intensity while the observations were being made; whereas Debbie was already a respectable hurricane that appeared to decrease in intensity while under observation. However, the authors must consider the radar problems and the distinct possibility that less echo tilt was noted in Debbie solely because the radar performance was below normal in comparison with the Betsy observations. Echo tilts computed by the authors from Heidi of 1967 were equal in magnitude to the Betsy tilts or about twice as great as the Debbie tilts.

## 10. CONCLUSIONS

Airborne radar photographs of hurricane Debbie were used to determine eye radius and echo-free area, major axis orientation, eye eccentricity, bright-band height and thickness, and precipitation tilt. The available PPI data on both days were used to make the eye size measurements at 5-min intervals beginning 1 hr before the first

seeding and ending 1 hr after the last seeding. Results for August 18th show sudden increases in echo-free area at seeding time plus 1 hr and 15 min. Area increases ranged from 50 percent to threefold.

Results for the 20th were quite different. A double eye structure was present on this day as opposed to a single eye on the 18th. The echo-free area within the smaller eye remained nearly constant throughout the day and the larger eye slowly decreased in area.

The only evidence of seeding effects on the 20th as noted from the radar photographs was observed in the rotation rate of the major axis of the elliptical eye. A slowing of the rotation rate was observed within 10 min of each seeding followed 1½ hr later by a rapid increase in the rotation rate that continued until the next seeding time. The period of this cycle (the time required for one revolution of the major axis) was about 2 hr, the same period as the seedings.

The changes in the radar eyewall radius were followed quite closely in time by changes in the radius of maximum winds. The hypothesis suggests that the large fluctuations observed on the 18th were due to seeding beyond the radius of maximum winds while the general lack, of such changes on the 20th might be attributed to seeding at smaller radii on that day. It is suggested, therefore, that, to obtain a more lasting modification of a storm, seeding be carried out more frequently, perhaps at 1-hr intervals and at successively larger radii as the eyewall expands. In the case of a storm with concentric wall clouds, seeding should probably be carried out beyond the outer wind maximum.

On the one day with usable RHI data, the echo tilts indicated that the shear is most often found in the lower levels of the storm. Most echoes leaned slightly backward, up spiral bands and radially outward as they increased in height. The average tilt was about 1 n.mi. horizontally in 3 n.mi. vertically, corresponding to a wind shear of 6 kt per 15,000 ft.

The bright band was found in most quadrants and at most ranges from the storm center. It was slightly higher near the eyewall than at the 100-n.mi. radius.

## ACKNOWLEDGMENTS

The authors gratefully thank the commander and personnel of U.S. Navy Weather Reconnaissance Squadron Four and the radar data advisors, without whose help and cooperation most of these data would not have been obtained.

The assistance of the dedicated people of the U.S. Air Force and NOAA-Research Flight Facility was also necessary in gathering some of the radar and other data used. Finally, thanks are due R. C. Gentry, Director of the National Hurricane Research Laboratory and Project Stormfury for his support and encouragement of this work.

## REFERENCES

- Atlas, David, Hardy, Kenneth R., Wexler, Raymond, and Boucher, Roland J., "On the Origin of Hurricane Spiral Bands," *Proceedings of the Third Technical Conference on Hurricanes and Tropical Meteorology, Mexico City, Mexico, June 6-12, 1963, Geofisica Internacional*, Vol. 3, No. 3/4, Mexico City, July/Dec. 1963, pp. 123-132.
- Battan, Louis J., *Radar Meteorology*, University of Chicago Press, Chicago, Ill., 1959, 161 pp. (see p. 96).
- Byers, Horace R., and Braham, Roscoe R., Jr., *The Thunderstorm*, U.S. Department of Commerce, Washington, D.C., June 1949, 287 pp.
- Fortner, Limon E., Jr., "Typhoon Sarah 1956," *Bulletin of the American Meteorological Society*, Vol. 39, No. 12, Dec. 1958, pp. 633-639.
- Fujita, Tetsuya T., The University of Chicago, Ill., July 1971 (personal communication).
- Fujita, Tetsuya T., and Black, Peter G., "In- and Outflow Field of Hurricane Debbie as Revealed by Echo and Cloud Velocities From Airborne Radar and ATS-III Pictures," *Proceedings of the Fourteenth Radar Meteorology Conference, Tucson, Arizona, November 17-20, 1970*, American Meteorological Society, Boston, Mass., 1970, pp. 353-358.
- Gentry, R. Cecil, "Project STORMFURY," *Bulletin of the American Meteorological Society*, Vol. 50, No. 6, June 1969, pp. 404-409.
- Gentry, R. Cecil, "Hurricane Debbie Modification Experiments, August 1969," *Science*, Vol. 168, No. 3930, Apr. 24, 1970, pp. 473-475.
- Gentry, R. Cecil, and Hawkins, Harry F., "A Hypothesis for the Modification of Hurricanes," *Project STORMFURY Annual Report, 1970*, Appendix B, Miami, Fla., May 1971, pp. B-1-B-15.
- Gunn, Ross, and Kinzer, Gilbert D., "The Terminal Velocity of Fall for Water Droplets in Stagnant Air," *Journal of Meteorology*, Vol. 6, No. 4, Aug. 1949, pp. 243-248.
- Hawkins, Harry F., "Comparison of Results of the Hurricane Debbie (1969) Modification Experiments With Those From Rosenthal's Numerical Model Simulation Experiments," *Monthly Weather Review*, Vol. 99, No. 5, May 1971, pp. 427-434.
- Hawkins, Harry F., and Rubsam, Daryl T., "Hurricane Hilda, 1964: I. Genesis, as Revealed by Satellite Photographs, Conventional and Aircraft Data," *Monthly Weather Review*, Vol. 96, No. 7, July 1968a, pp. 428-452.
- Hawkins, Harry F., and Rubsam, Daryl T., "Hurricane Hilda, 1964: II. Structure and Budgets of the Hurricane on October 1, 1964," *Monthly Weather Review*, Vol. 96, No. 9, Sept. 1968b, pp. 617-636.
- Hoecker, Walter, and Brier, Glenn, "Measurement of Hurricane Eye Diameter by Land-Based and Airborne Radar," Air Resources Laboratory, NOAA, Washington, D.C., 1970 (personal communication).
- Jordan, Charles L., and Schatzle, Frank J., "Weather Note—The 'Double Eye' of Hurricane Donna," *Monthly Weather Review*, Vol. 89, No. 9, Sept. 1961, pp. 354-356.
- Malkus, Joanne S., Ronne, Claude, and Chaffee, Margaret, "Cloud Patterns in Hurricane Daisy, 1958," *Tellus*, Vol. 13, No. 1, Feb. 1961, pp. 8-30.
- Mueller, E. A., and Jones, D. M. A., "Drop-Size Distributions in Florida," *Proceedings of the Eighth Weather Radar Conference, San Francisco, California, April 11-14, 1960*, American Meteorological Society, Boston, Mass., 1960, pp. 299-305.
- Rosenthal, Stanley L., "A Circularly Symmetric Primitive Equation Model of Tropical Cyclone Development Containing an Explicit Water Vapor Cycle," *Monthly Weather Review*, Vol. 98, No. 9, Sept. 1970, pp. 643-663.
- Rosenthal, Stanley L., "A Circularly Symmetric, Primitive Equation Model of Tropical Cyclones and Its Response to Artificial Enhancement of the Convective Heating Function," *Monthly Weather Review*, Vol. 99, No. 5, May 1971, pp. 414-426.
- Sadowski, Alexander, "Radar Analysis of Hurricane Donna's Recurvature," *Proceedings of the Second Technical Conference on Hurricanes, Miami Beach, Florida, June 27-30, 1961*, National Hurricane Research Laboratory, U.S. Weather Bureau, Miami, Fla., Mar. 1962, pp. 63-69.
- Senn, Harry V., "Radar Hurricane Precipitation Patterns as Track Indicators," *Proceedings of the Twelfth Conference on Radar Meteorology, Norman, Oklahoma, October 17-20, 1966*, American Meteorological Society, Boston, Mass., 1966a, pp. 436-440.
- Senn, Harry V., "Precipitation Shear and Bright Band Observations in Hurricane Betsy 1965," *Proceedings of the Twelfth Conference on Radar Meteorology, Norman, Oklahoma, October 17-20, 1966*, American Meteorological Society, Boston, Mass., 1966b, pp. 447-453.
- Senn, Harry V., and Hiser, Homer W., "Effectiveness of Various Radars in Tracking Hurricanes," *Proceedings of the Second Technical Conference on Hurricanes, Miami Beach, Florida, June 27-30, 1961*, National Hurricane Research Laboratory, U.S. Weather Bureau, Miami, Fla., Mar. 1962, pp. 101-114.
- Sheets, Robert C., National Hurricane Research Laboratory, NOAA, Coral Gables, Fla., Sept. 1970 (personal communication).
- Simpson, Robert H., Ahrens, Merle R., and Decker, Richard D., "A Cloud Seeding Experiment in Hurricane Esther, 1961," *National Hurricane Research Project Report No. 60*, U.S. Weather Bureau, Washington, D.C., Apr. 1963, 30 pp.
- Simpson, Robert H., and Malkus, Joanne S., *Hurricane Modification: Progress and Prospects, 1964*, U.S. Weather Bureau, Washington, D.C., Aug. 1964, 54 pp.
- United States Navy Fleet Weather Facility, *STORMFURY Operations Plan No. 1-69*, Naval Air Station, Jacksonville, Fla., June 1969, 100 pp.

[Received March 29, 1971; revised August 26, 1971]